ACS APPLIED MATERIALS & INTERFACES

Research Article

www.acsami.org

Amide Functionalized Microporous Organic Polymer (Am-MOP) for Selective CO_2 Sorption and Catalysis

Venkata M. Suresh,[†] Satyanarayana Bonakala,[‡] Hanudatta S. Atreya,[§] Sundaram Balasubramanian,[‡] and Tapas Kumar Maji*,[†]

[†]Molecular Materials Laboratory, [‡]Molecular Simulations Laboratory, Chemistry & Physics of Materials Unit, Jawaharlal Nehru Centre for Advanced Scientific Research, Jakkur-560064, Bangalore, Karnataka, India

[§]NMR Research Centre, Indian Institute of Science, Bangalore, 560012 Karnataka, India

Supporting Information

ABSTRACT: We report the design and synthesis of an amide functionalized microporous organic polymer (**Am-MOP**) prepared from trimesic acid and *p*-phenylenediamine using thionyl chloride as a reagent. Polar amide (−CONH−) functional groups act as a linking unit between the node and spacer and constitute the pore wall of the continuous polymeric network. The strong covalent bonds between the building blocks (trimesic acid and *p*-phenylenediamine) through amide bond linkages provide high thermal and chemical stability to **Am-MOP**. The presence of a highly polar pore surface allows selective CO_2 uptake at 195 K over other gases such as N_2, Ar, and O_2. The CO_2 molecule interacts with amide functional groups via Lewis acid−base type interactions as demonstrated through DFT calculations. Furthermore, for the first time **Am-MOP** with basic functional groups has been exploited for the Knoevenagel condensation reaction between aldehydes and active methylene compounds. Availability of a large number of catalytic sites per volume and confined microporosity gives enhanced catalytic efficiency and high selectivity for small substrate molecules.

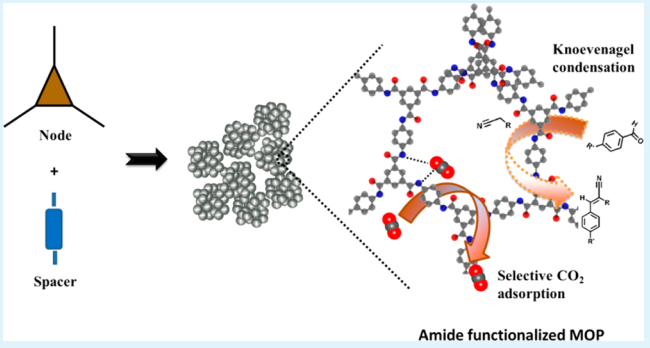

KEYWORDS: *porous organic polymer, microporosity, polar pore surface, CO_2 adsorption, Knoevenagel condensation, catalysis*

1. INTRODUCTION

Design and synthesis of microporous organic polymers (MOPs) with pore size <2 nm have attracted tremendous attention in both academia and industry owing to their potential applications in gas storage,[1−4] separation,[5−7] opto-electronics,[8−10] and catalysis.[11−14] The presence of light elements (C, H, N, and O) makes them extremely less dense than known porous materials. The vast choice of organic building blocks and synthetic diversity allow fine-tuning of the pore surface and specific surface area of the polymers, and strong covalent bonding in the network would lead to high thermal and chemical stability.[15,16]Although metal−organic frameworks (MOFs) are recognized for high specific surface areas and adsorption capacities,[17,18] limited hydrolytic stability of most of the MOFs (excluding few stable MOFs such as zeolitic imidazolate frameworks (ZIFs) and Materials of Institute Lavoisier (MILs)) restrict their applications in humid or other extreme conditions.[19] In this regard, organic polymers are superior porous materials with a greater degree of recyclability.[20−22] Specifically, selective CO_2 capture and storage has gained a lot of interest due to its environmental, economic reasons, and separation of CO_2 from N_2 is one of the prime requirements for the CO_2 capture technology with concern of flue gas. Apart from MOFs,[23−27] several MOPs have also been studied for selective CO_2 sorption.[28−30] CO_2 sorption capacity does not solely depend on the surface area, functionalities such as $-NH_2$, −C═N, −OH, F, etc. present on the pore surface which tune the isosteric heats of adsorption required to attain higher amount of uptake and selectivity in microporous frameworks either in MOFs or organic porous polymers.[31−36] However, the costly metal complex catalysts associated in the case of conjugated microporous polymers (CMPs), reversible nature of imine bonds in covalent organic frameworks (COFs), or limited stability of MOFs at high temperature conditions limit their usage. Therefore we sought to design MOPs with simple building blocks having basic polar functionalities for improving CO_2 selectivity and other properties like catalysis. With this objective, we have designed a new microporous organic polymer with amide (>CONH) functional groups (**Am-MOP**) on the pore surface and envisage that these amide groups would specifically interact with CO_2 molecules having a large quadrupole moment and the mildly

Received: August 16, 2013
Accepted: March 18, 2014
Published: March 18, 2014

Scheme 1. Schematic for Synthesis of Am-MOP Polymer

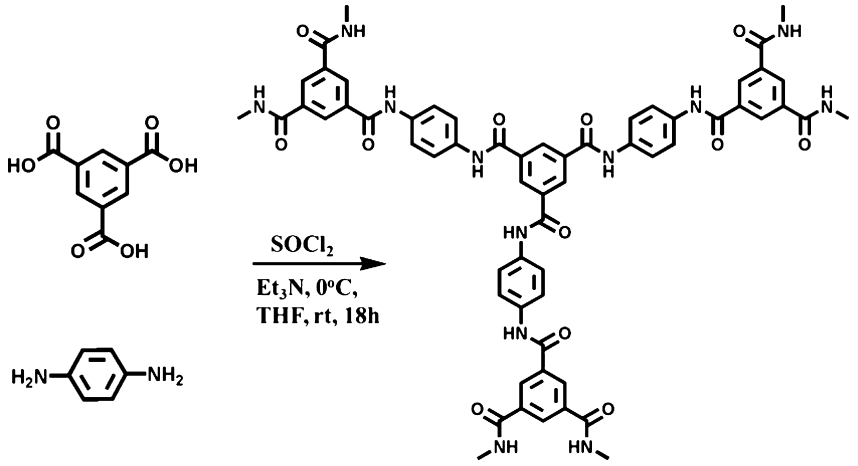

basic nature of amide groups could be exploited for heterogeneous catalysis. In this contribution, we report the design and synthesis of an amide functionalized organic polymer (**Am-MOP**) based on condensation of trimesic acid and *p*-phenylenediamine and characterized by FTIR, ^{13}C/CP-MAS NMR, FESEM, TEM, and PXRD measurements. **Am-MOP** shows inherent microporosity and selective CO_2 uptake over other gases. Moreover, inherent microporosity of **Am-MOP** with mild basic functional groups prompted us to study catalytic Knoevenagel condensation reactions. The high density of amide groups along the pore walls, inherent H-bonding capability with different organic molecules, and confined microporosity result in facile interaction with the substrates and give enhanced selectivity and high catalytic efficiency.

2. EXPERIMENTAL SECTION

2.1. Materials. 1,3,5-Benzenetricarboxylic acid or trimesic acid and *p*-phenylenediamine were purchased from Sigma Aldrich Chemical Co. and used without further purification. All solvents were dried before using. Triethylamine, aniline, thionyl chloride, and all reagents used for catalysis were purchased from Across Organics.

2.2. Characterization. The elemental analysis was carried out using Thermo Fischer Flash 2000 Elemental Analyzer. Infrared (IR) spectra were carried out using KBr pellets on a Bruker FT-IR spectrometer. Solid-state ^{13}C cross-polarization magnetic angle spinning (CP-MAS) NMR spectra were measured on a Varian Infinity Plus 300 WB spectrometer at a MAS rate of 5 kHz and a CP contact time of 1.4 ms. Morphological studies have been carried out using Lica-S440I field emission scanning electron microscopy (FESEM) by placing samples on a silicon wafer under high vacuum with an accelerating voltage of 10 kV. Transmission electron microscopy (TEM) analysis was carried on a JEOL JEM-3010 transmission electron microscope with an accelerating voltage of 300 kV. The sample is prepared by dispersing **Am-MOP** in ethanol under sonication and drop casted onto a carbon-coated copper grid. Powder X-ray diffraction (PXRD) measurements were carried out using Bruker Discover-8 diffractometer employing Cu−Kα radiation. Thermogravimetric analysis (TGA) was done using Mettler Toledo TGA 850 instrument in nitrogen atmosphere in the range of 30−800 °C with a heating rate of 5 °C per min. Porosity measurements were accomplished using QUNATACHROME QUADRASORD-SI analyzer at 77 K for N_2, 195 K for CO_2, Ar, N_2, and H_2 at low pressure and for CO_2 at 273 K, 293 K, and 1 atm.

2.3. Synthesis of Am-MOP. In a typical experiment trimesic acid (1 equiv, 105.07 mg) in tetrahydrofuran (THF) within a Schlenk flask is degassed and purged with argon (Ar). To this thionyl chloride (3.5 equiv, 0.127 mL) was added dropwise under the continuous flow of Ar. The mixture is allowed to heat at 80 °C for 2 h. After cooling the mixture to room temprature, it was washed with dry THF several times resulting in trimesoyl chloride. To trimesoyl chloride in dry THF, a solution of *p*-phenylenediamine (1.5 equiv, 81.0 mg) and triethylamine (1.5 equiv, 0.1 mL) in THF was added dropwise at 0 °C under continuous stirring. The reaction is allowed to cool to room temperature and further stirred for 18 h. The precipitates were collected by filtration and washed several times with THF, water, and acetone. The resultant powder immersed in acetone overnight and dried at room temperature under vacuum to afford a pale white powder. Yield: 75%. Elemental analysis of guest free samples for $C_{27}H_{21}N_6O_3$ Calculated: C, 67.9; H, 4.4; N, 17.6. Found: C, 63.3; H, 5.0; N, 13.2. FT-IR (cm^{-1}): 3243 (br), 3066 (br), 1664 (sh), 1511 (sh), 1403 (sh), 1309 (sh), 1246 (sh), 829 (sh), 791 (w), 518 (br).

2.4. General Procedure for the Catalytic Reactions. Benzaldehyde derivative (1 equiv) and malononitrile (1 equiv) were taken in a predried Schlenk tube, and THF (3 mL) was added to it under inert atmosphere. It is stirred for ten minutes at room temperature followed by the addition of guest free **Am-MOP** (0.9 mol %). The reaction mixture is refluxed at 40 °C under nitrogen atmosphere. The reaction mixture is concentrated and filtered to recover the catalyst. Filtrate is analyzed using a GC-MS analyzer, and products were qualitatively analyzed by ^1H NMR spectroscopy (see the Supporting Information for details).

2.5. Computational Details. Geometry optimization of a basic unit (Figure 5a) was carried out in gas phase using Gaussian 09.[37] The initial structure was modeled in GaussView[38] which was optimized for its geometry at the M06-2X/cc-pvtz level of theory. The dimer (Figure 5b) of the basic unit was optimized at the M06-2X/cc-pvdz level of theory. During the geometry optimization, the maximum component of force on any atom was converged to less than 4.5×10^{-5} au.

As seen in Figure 5b, the amide groups can form hydrogen bonds among themselves in the native **Am-MOP**; thus the adsorbed CO_2 will interact through weak Lewis acid/base interaction with the carbonyl oxygen of the amide. The binding energy of CO_2 with the dimer of a basic unit (Figure 7b) was calculated using the M06-2X/cc-pvdz//M06-2X/cc-pvtz level of theory as follows

$$\Delta E = E_{\text{basic unit+CO2}} - E_{\text{basic unit}} - E_{\text{CO2}}$$

where ΔE = binding energy of CO_2, $E_{\text{basic unit+CO2}}$ = optimized energy of basic unit with CO_2, $E_{\text{basic unit}}$ = optimized energy of basic unit, and E_{CO2} = optimized energy of CO_2.

To know the types of interactions exhibit by CO_2, we calculated electron density difference maps using the M06-2X/cc-pvtz level of theory. It is calculated as

$$\Delta\rho = \rho_{\text{basic unit+CO2}} - \rho_{\text{basic unit}} - \rho_{\text{CO2}}$$

where $\Delta\rho$ = difference in electron density, $\rho_{\text{basic unit+CO2}}$ = total electron density of basic unit with CO_2, $E_{\text{basic unit}}$ = total electron density of

dx.doi.org/10.1021/am500057z | ACS Appl. Mater. Interfaces 2014, 6, 4630−4637

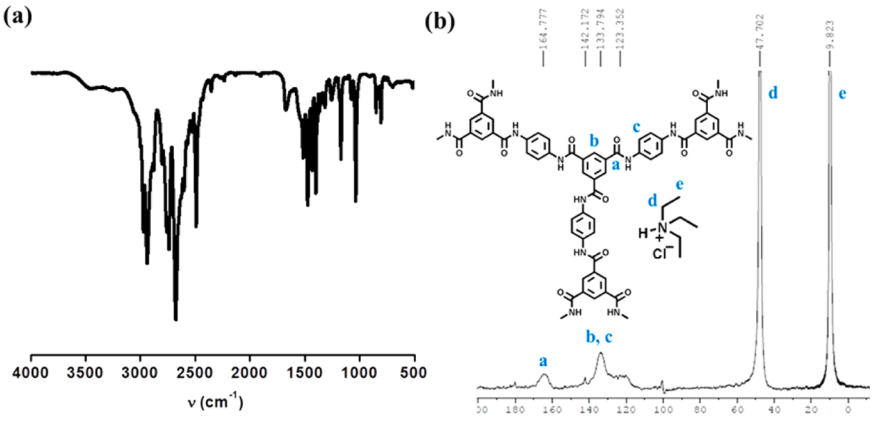

Figure 1. (a) FTIR spectra of as-synthesized **Am-MOP** and (b) solid-state ^{13}C/CP-MAS NMR of as-synthesized **Am-MOP** showing the presence of triethylammonium chloride salt.

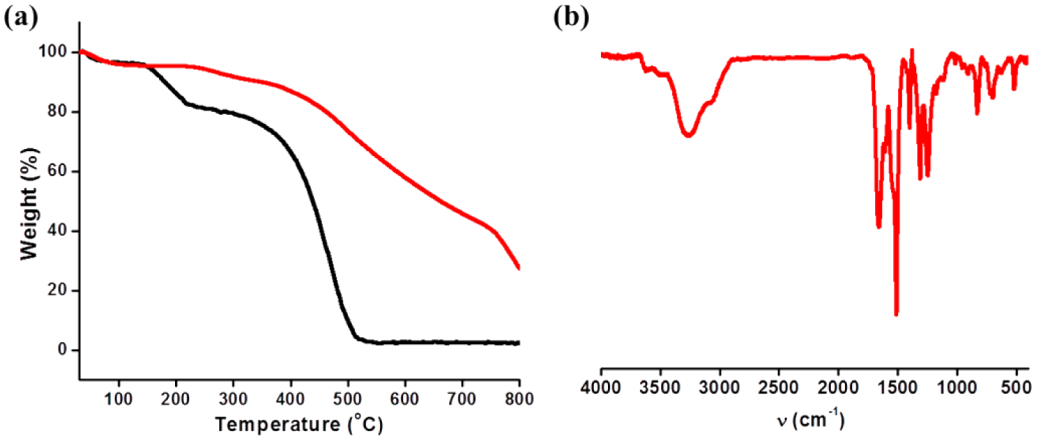

Figure 2. (a) TGA of as-synthesized (black) and guest free (red) **Am-MOP** with a heating rate of 5 °C/min in the range of 30−800 °C and (b) FTIR spectra of guest free **Am-MOP** indicating the intact of amide linkage in the polymer.

basic unit, and E_{CO2} = total electron density of CO_2. All structures were visualized using GaussView and VMD.[39]

The binding energy was calculated to be −28.4 kJ/mol using the M06-2X/cc-pvdz//M06-2X/cc-pvtz level of theory.

3. RESULTS AND DISCUSSION

3.1. Structural Characterization. The polymer **Am-MOP** is reproducibly synthesized by the condensation of trimesic acid and *p*-phenylenediamine in tetrahydrofuran (THF) using thionyl chloride and triethylamine (Scheme 1). The as-synthesized **Am-MOP** has been characterized by Fourier transform infrared spectroscopy (FTIR), solid-state ^{13}C/CP-MAS NMR, and thermogravimetric analysis (TGA). FTIR of **Am-MOP** shows bands at 1673 cm^{-1} and 3270 cm^{-1} corresponding to ν(C═O) and ν(N−H) stretching vibrations of amide bond indicating condensation of *p*-phenylenediamine and trimesic acid. The presence of strong peaks in the range of 2677−2934 cm^{-1} was attributed to aliphatic alkyl chains of the triethylammonium chloride salt (formed by the reaction of Et_3N and HCl during the course of polymer formation) present in the pores of the polymer. Peaks at 1514 cm^{-1} and 1398 cm^{-1} can be attributed to ν(N−H) in-plane bending and ν(C−N) stretching vibrations of amide groups (Figure 1a). Further, the presence of amide functional groups in **Am-MOP** is confirmed by the presence of peaks at 164 ppm in solid-state ^{13}C/CP-MAS NMR spectra, and all other peaks ranging from 120 to 140 ppm correspond to aromatic carbons and peaks at 47 ppm and 10 ppm could be attributed to the aliphatic carbons of in situ generated triethylammonium chloride present inside the pores as a guest or template molecules (Figure 1b). Also, TGA analysis shows weight loss of 13% between 150 and 200 °C which corresponds to the loss of triethylammonium chloride entrapped in the pores and further heating shows no loss up to 400 °C indicating the high thermal stability of **Am-MOP** (Figure 2a, black). Hence, the sample was evacuated at 200 °C in a long glass tube used for adsorption measurement, where we observed crystalline transparent salts condensed at the upper part of the tube during degassing and is confirmed to be triethylammonium chloride salt from ^{1}H NMR and powder X-ray diffraction measurements (Figures S1 and S2). The sample is completely evacuated at 200 °C for 72 h under vacuum to remove all the salt present in the pores of **Am-MOP**. TGA analysis of a guest free sample shows a weight loss of 2% below 100 °C attributed to loss of moisture in **Am-MOP** (Figure 2a, red). Elemental analysis of guest free **Am-MOP** is found to be $C_{27}H_{21}N_6O_3(H_2O)_2$ which is closely matching with the monomer unit of polymer with little moisture as observed in TGA analysis. Guest free **Am-MOP** is further characterized by FT-IR, ^{13}C/CP-MAS solid-state NMR, and powder X-ray diffraction (PXRD) studies. FTIR of **Am-MOP** shows bands at 1664 cm^{-1} and 3270 cm^{-1} corresponding to ν(C═O) and ν(N−H) stretching of an amide bond indicating the amide linkage in the polymer is intact even after complete removal of salt at 200 °C (Figure 2b). Further, the presence of amide

dx.doi.org/10.1021/am500057z | ACS Appl. Mater. Interfaces 2014, 6, 4630−4637

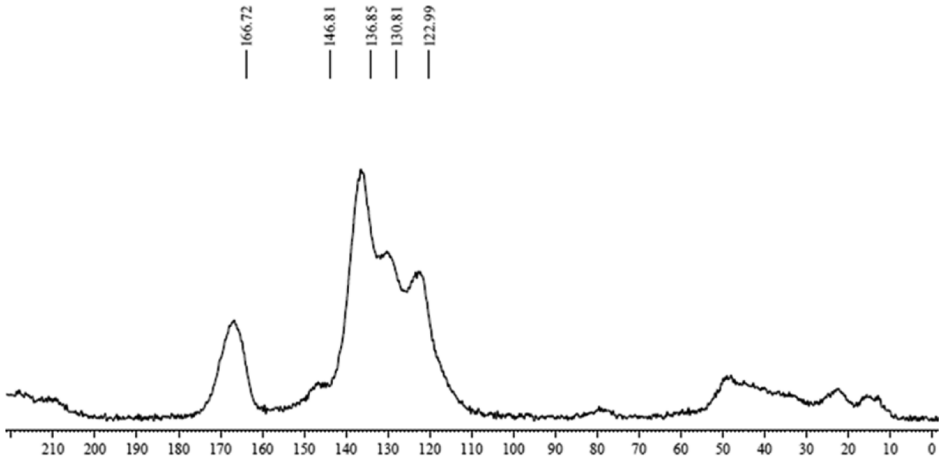

Figure 3. Solid-state ^{13}C/CP-MAS NMR of guest free **Am-MOP** indicating the absence of any salt impurities.

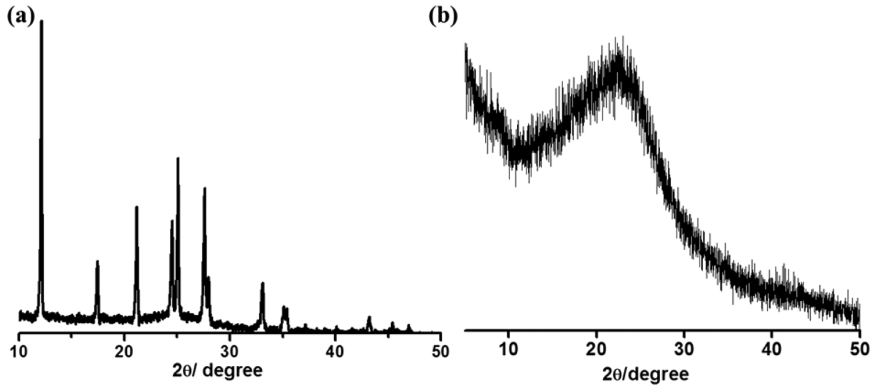

Figure 4. Powder X-ray diffraction patterns of (a) as-synthesized and (b) guest free **Am-MOP**.

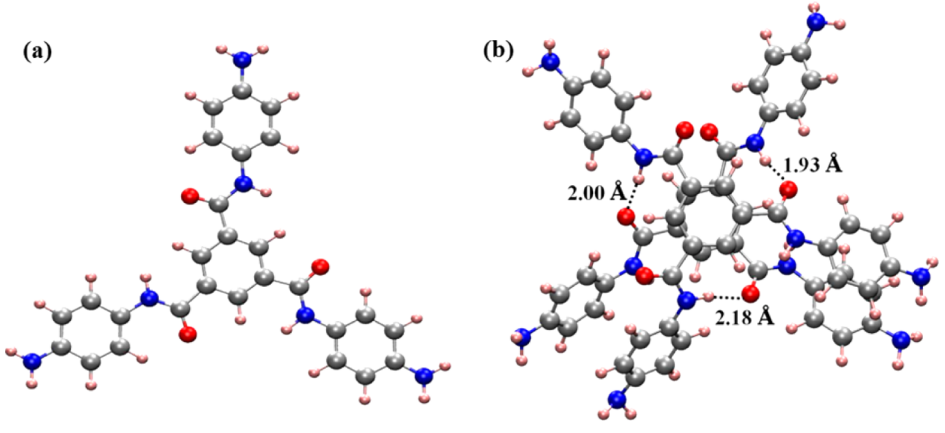

Figure 5. Optimized geometry of (a) basic unit and (b) a dimer of the basic unit. C - silver, H - pink, N - blue, O - red.

functional groups in **Am-MOP** is confirmed by the presence of signals at 166 ppm with enhanced intensity in ^{13}C/CP-MAS solid-state NMR spectra in comparison to as-synthesized **Am-MOP** (Figure 3), and the absence of any peaks at 47 ppm and 10 ppm indicates that triethylammonium chloride is completely removed from the polymer. PXRD measurements of as-synthesized **Am-MOP** are observed to be crystalline which is corroborated to triethylammonium chloride salt, and guest free sample shows a broad peak centered at 24° suggesting that the guest free polymer is amorphous in nature (Figures 4a and 4b).

The basic unit as shown in Scheme 1 was optimized for its geometry using density functional theory (see the Experimental Section), and the same is shown in Figure 5a. This C3 symmetric moiety is planar. However, in a laterally stacked dimer, such units became nonplanar due to the formation of several N−H···O hydrogen bonds (Figure 5b). The formation of hydrogen bonds has been shown to induce a red shift in the carbonyl and N−H stretching frequencies in the literature.[40,41] We too have observed such a red shift in these bands, relative to their gas phase values suggesting the H-bonding between the units.

3.2. Morphology and Porosity. Morphology of the **Am-MOP** was investigated using field emission scanning electron microscopy (FESEM). At low magnifications compound shows

dx.doi.org/10.1021/am500057z | ACS Appl. Mater. Interfaces 2014, 6, 4630−4637

aggregation of small particles resulting in irregular morphology (Figure 6a). Further magnification shows the presence of

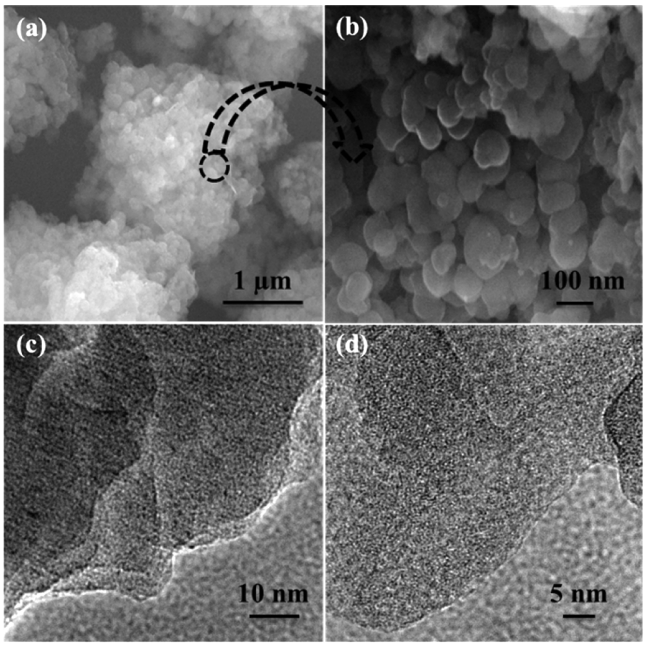

Figure 6. (a), (b) FESEM images of **Am-MOP** at different magnifications showing spherical particles and (c), (d) TEM images of **Am-MOP** showing continuous microporous polymer networks.

spherical particles clustered together and undergoes agglomeration which is prevalent in several microporous organic polymers,[42] and the particle size ranges from 50 to 200 nm (Figure 6b). Interestingly, TEM image analysis of **Am-MOP** shows that these spherical particles constitute an extended network structure (Figure 6c). Further magnification at the edges of these particles discloses the presence of continuous microporous structure (Figure 6d). Many covalent organic frameworks reported in the literature possess sheetlike morphologies and whose XRD pattern have been modeled using stacked sheets with hexagonal network topologies.[43,44] However, the formation of strong hydrogen bonds between the amide groups of two basic units (as seen in Figure 5) promotes nonplanar, three-dimensional architectures. Thus, both the experimental and theoretical data strongly suggest this **Am-MOP** to be an extended three-dimensional porous network than one constituted by two-dimensional sheets.

The permanent porosity of completely guest free **Am-MOP** was analyzed using adsorption experiments with different adsorbates. The guest free sample is activated at 150 °C to remove any moisture prior to the adsorption measurements. Adsorption measurements of N_2 (kinetic diameter = 3.6 Å) carried out at 77 K show a typical type-II profile suggesting the surface adsorption (Figure 7a) and nonporous nature of polymer to N_2. Interestingly, an appreciable amount of CO_2 (kinetic diameter = 3.3 Å) adsorption was observed at 195 K with a typical type-I profile, reflecting the microporous nature (<2 nm) of the polymer. The final amount of CO_2 adsorbed is found to be 40 mL/g which corresponds to 0.8 molecules per formula unit (Figure 7a) and the Langmuir surface area calculated to be 223 m^2/g. Further, no uptake of other gases like H_2 (2.89 Å), Ar (3.7 Å), and N_2 (3.6 Å) is observed (Figure S3) at 195 K suggesting that the polymer is CO_2 selective. An optimized geometry of the CO_2 complexed with the dimer of the basic unit is displayed in Figure 7b. The geometry was obtained within the M06-2X[45]/cc-pvdz level of theory, and the binding energy of CO_2 was calculated as −28.4 kJ/mol at the M06-2X/cc-pvtz//M06-2X/cc-pvdz level of theory. This value is comparable to the experimental heat of enthalpy −27.6 kJ/mol calculated using the Dubinin−Radushkevich (DR) equation[46] at 195 K. Electron density difference map analysis shows that CO_2 interacts via Lewis acid−base type interaction with the oxygen of amide carbonyl and also undergoes weak H-bonding interaction with the phenyl C−H and $\pi-\pi$ interactions with the aromatic phenyl group. We have further studied the CO_2 uptake capacity of **Am-MOP** at 273 K and 1 atm. As shown in Figure S4, **Am-MOP** shows a type-I CO_2 uptake profile with the final amount being about 20 mL/g. Similar uptake amounts are also reported in other organic microporous polymers at similar conditions.[47,48] We have calculated the pore size distribution of **Am-MOP** from CO_2 adsorption data at 273 K using the density functional theory (DFT) method.[49] The pore width distribution showed maxima at 3.0 and 4.1 Å (Figure S5) suggesting the microporous nature of the polymer.

3.3. Catalysis. Amide is a fascinating functional group attributed for its dual interaction sites through the −NH moiety and the >C═O group. The mildly basic nature of the amide

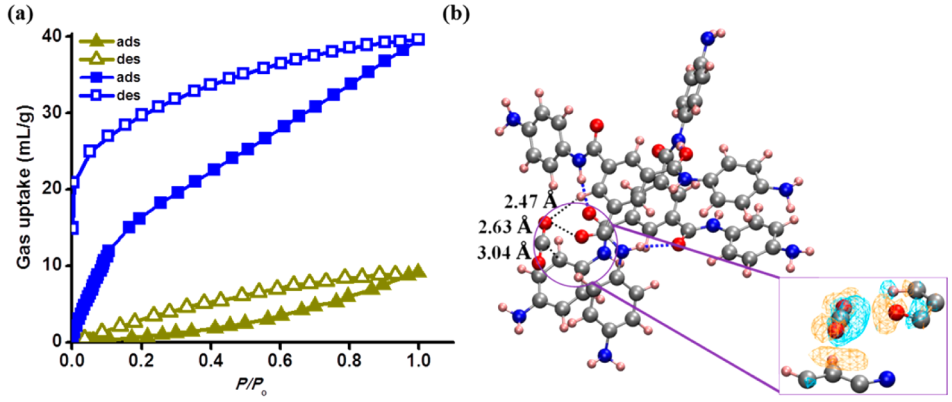

Figure 7. Adsorption isotherms of **Am-MOP** (a) N_2 at 77 K (yellow) and CO_2 at 195 K (blue). (b) Optimized geometry of the basic unit complexing with CO_2. Cyan and orange regions indicate decreased and increased electron densities, respectively. The isosurface value is 5×10^{-4} au. C - silver, H - pink, N - blue, O - red.

dx.doi.org/10.1021/am500057z | ACS Appl. Mater. Interfaces 2014, 6, 4630−4637

functional group makes it versatile in catalyzing the condensation reactions. For instance Kitagawa et al. and Zhou et al. recently reported the Knoevenagel condensation reaction using three-dimensional porous coordination polymers with amide functional groups immobilized on the pore walls.[50,51] The interlinking amide groups constituting the pore wall of the **Am-MOP** prompted us to study its catalytic activity toward condensation of aldehydes and active methylene compounds (commonly known as Knoevenagel condensation).

Malononitrile and *p*-nitrobenzaldehyde were taken as reference to test the catalytic activity of activated guest free **Am-MOP**. In a typical condensation reaction *p*-nitrobenzaldehyde (1 equiv), malononitrile (1 equiv), and **Am-MOP** (0.9 mol %) were taken in dry THF and stirred at 40 °C under inert atmosphere conditions (Figure 8). The quantitative analysis of

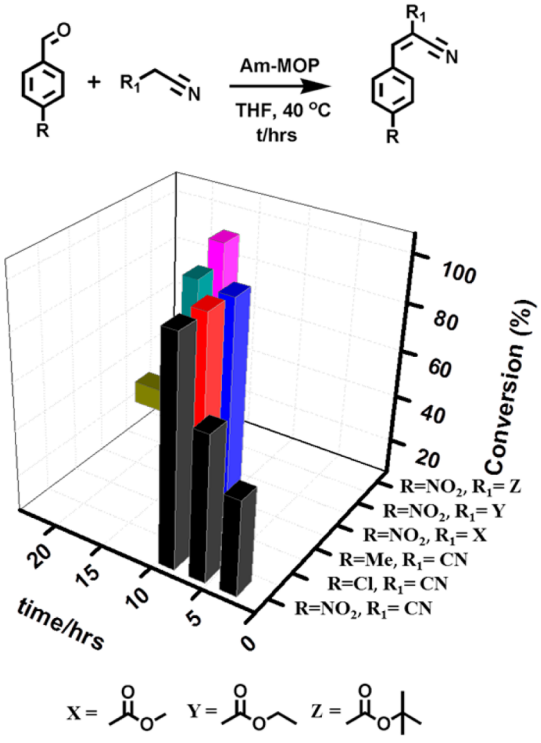

Figure 8. Catalytic reactions of the Knoevenagel condensation using guest free **Am-MOP** and a conversion profile for various aldehydes and active methylene compounds.

the product is monitored using GC-MS analyzer at regular intervals of time. Although low conversion (37%) of conjugated enone is observed in the first 3 h (Figure S6), a steep increase has been noticed in the next few hours (66%, 6 h) (Figure S7), and almost all the benzaldehyde is converted to product within 9 h (>99%) (Figure S8). With this result, we are encouraged to study the catalytic efficiency of **Am-MOP** toward different active methylene compounds, and conversion results are summarized in Figure 8. In order to check the selectivity of the **Am-MOP**, we have chosen the bulkier methyl and ethyl cyano acetate. Interestingly, appreciable conversions were observed, in the case of the methyl derivative (88%) and up to 90% conversion in the case of ethyl cyano acetate. However, the reaction takes a longer time (about 12 h compared to malononitrile), and no selectivity was observed between malononitrile and methyl or ethyl cyano acetate. It is noteworthy to mention, the longer reaction times in the case of methyl and ethyl substituted active methylene compounds suggest that the network has the possibility to swell slowly in order to accommodate the active methylene precursor and catalyze the reaction. The swelling of polymer network in organic solvents is often observed in microporous organic polymers.[52] On the other hand, the catalytic reaction with the much bulkier *tert*-butylcyanoacetate shows feeble (<15%) conversion under similar conditions even after 24 h. These results suggest that **Am-MOP** is selective for small molecules, and the large size of the *tert*-butyl precursor could not pass through the pore window. These results suggest that the micropore size of the catalyst plays an important role in enhancing the selectivity of the Knoevenagel condensation reaction. The catalytic reaction between malononitrile and *p*-nitrobenzaldehyde using triphenylbenzamide (basic unit, prepared by the condensation of trimesoylchloride and aniline, Figure S9) shows no appreciable conversion (<10%) even after 24 h suggesting the efficiency of **Am-MOP** in catalyzing the reaction. Products formed using catalytic **Am-MOP** was analyzed by ^{1}H NMR analysis (Figures S10−S13). The enhanced efficiency of **Am-MOP** may be attributed to a large number of catalytic sites available per volume, and micropore confinement of the substrate would expect to play a role along with basicity of amide functionality in enhancing the reaction yields. Catalytic efficiency of **Am-MOP** is observed to be similar up to four cycles of catalytic reactions.

4. CONCLUSIONS

In conclusion, we have successfully demonstrated the molecular design and synthesis of an amide functionalized organic polymer with microporosity. The presence of polar amide functional groups along the pore wall displays high selectivity in CO_2 uptake through effective interaction of CO_2 with the >CONH group as supported by DFT based calculations. Furthermore, mild basic functionalities (>CONH) were exploited for Knoevenagel condensation reactions with good selectivity. This work would pave the way to fabricate amide functionalized polymers with tunable porosity depending on the length of the linker with enhanced surface area, CO_2 uptake, and catalytic activity.

■ ASSOCIATED CONTENT

Ⓢ Supporting Information

^{1}H NMR spectra and PXRD pattern of triethylammonium chloride, CO_2 selectivity at 195 K and CO_2 uptake capacity (273 K and 1 atm) of **Am-MOP** polymer, pore-size distribution of **Am-MOP** calculated using the DFT model. GC-MS spectra of **Am-MOP** catalysis for nitrobenzaldehyde, ^{1}H NMR spectra of basic unit and condensation product of **Am-MOP** catalytic reactions. This material is available free of charge via the Internet at http://pubs.acs.org.

■ AUTHOR INFORMATION

Corresponding Author

*E-mail: tmaji@jncasr.ac.in.

Notes

The authors declare no competing financial interest.

■ ACKNOWLEDGMENTS

We thank Prof. C. N. R. Rao for his support and encouragement. We acknowledge Selvi (FESEM) and Usha (TEM) for microscopic measurements. M.V.S. and S. Bonakala

thank CSIR (Govt. of India) for a fellowship. T.K.M. and S. Balasubramanian gratefully acknowledge Sheikh Saqr a fellowship.

REFERENCES

(1) Dawson, R.; Laybourn, A.; Khimyak, Y. Z.; Adams, D. J.; Cooper, A. I. High Surface Area Conjugated Microporous Polymers: The Importance of Reaction Solvent Choice. *Macromolecules* **2010**, *43*, 8524−8530.

(2) Hauser, B. G.; Farha, O. K.; Exley, J.; Hupp, J. T. Thermally Enhancing the Surface Areas of Yamamoto-Derived Porous Organic Polymers. *Chem. Mater.* **2013**, *25*, 12−16.

(3) McKeown, N. B.; Budd, P. M. Polymers of Intrinsic Microporosity (PIMs): Organic Materials for Membrane Separations, Heterogeneous Catalysis and Hydrogen Storage. *Chem. Soc. Rev.* **2006**, *35*, 675−683.

(4) Xu, S.; Luo, Y.; Tan, B. Recent Development of Hypercrosslinked Microporous Organic Polymers. *Macromol. Rapid Commun.* **2013**, *34*, 471−484.

(5) Lu, W.; Yuan, D.; Zhao, D.; Schilling, C. I.; Plietzsch, O.; Muller, T.; Braese, S.; Guenther, J.; Bluemel, J.; Krishna, R.; Li, Z.; Zhou, H.-C. Porous Polymer Networks: Synthesis, Porosity, and Applications in Gas Storage/Separation. *Chem. Mater.* **2010**, *22*, 5964−5972.

(6) Chang, Z.; Zhang, D.-S.; Chen, Q.; Bu, X.-H. Microporous Organic Polymers for Gas Storage and Separation Applications. *PCCP Phys. Chem. Chem. Phys.* **2013**, *15*, 5430−5442.

(7) Katsoulidis, A. P.; Kanatzidis, M. G. Mesoporous Hydrophobic Polymeric Organic Frameworks with Bound Surfactants. Selective Adsorption of C_2H_6 versus CH_4. *Chem. Mater.* **2012**, *24*, 471−479.

(8) Jiang, J.-X.; Trewin, A.; Adams, D. J.; Cooper, A. I. Band Gap Engineering in Fluorescent Conjugated Microporous Polymers. *Chem. Sci.* **2011**, *2*, 1777−1781.

(9) Chen, L.; Honsho, Y.; Seki, S.; Jiang, D. Light-Harvesting Conjugated Microporous Polymers: Rapid and Highly Efficient Flow of Light Energy with a Porous Polyphenylene Framework as Antenna. *J. Am. Chem. Soc.* **2010**, *132*, 6742−6748.

(10) Chen, Q.; Wang, J.-X.; Yang, F.; Zhou, D.; Bian, N.; Zhang, X.-J.; Yan, C.-G.; Han, B.-H. Tetraphenylethylene-Based Fluorescent Porous Organic Polymers: Preparation, Gas Sorption Properties and Photoluminescence Properties. *J. Mater. Chem.* **2011**, *21*, 13554−13560.

(11) Kaur, P.; Hupp, J. T.; Nguyen, S. T. Porous Organic Polymers in Catalysis: Opportunities and Challenges. *ACS Catal.* **2011**, *1*, 819−835.

(12) Shultz, A. M.; Farha, O. K.; Hupp, J. T.; Nguyen, S. T. Synthesis of Catalytically Active Porous Organic Polymers from Metalloporphyrin Building Blocks. *Chem. Sci.* **2011**, *2*, 686−689.

(13) Jiang, J.-X.; Wang, C.; Laybourn, A.; Hasell, T.; Clowes, R.; Khimyak, Y. Z.; Xiao, J.; Higgins, S. J.; Adams, D. J.; Cooper, A. I. Metal−Organic Conjugated Microporous Polymers. *Angew. Chem., Int. Ed.* **2011**, *50*, 1072−1075.

(14) Hug, S.; Tauchert, M. E.; Li, S.; Pachmayr, U. E.; Lotsch, B. V. A Functional Triazine Framework Based on N-Heterocyclic Building Blocks. *J. Mater. Chem.* **2012**, *22*, 13956−13964.

(15) Pandey, P.; Farha, O. K.; Spokoyny, A. M.; Mirkin, C. A.; Kanatzidis, M. G.; Hupp, J. T.; Nguyen, S. T. A "Click-Based" Porous Organic Polymer from Tetrahedral Building Blocks. *J. Mater. Chem.* **2011**, *21*, 1700−1703.

(16) Ren, S.; Bojdys, M. J.; Dawson, R.; Laybourn, A.; Khimyak, Y. Z.; Adams, D. J.; Cooper, A. I. Porous, Fluorescent, Covalent Triazine-Based Frameworks via Room-Temperature and Microwave-Assisted Synthesis. *Adv. Mater.* **2012**, *24*, 2357−2361.

(17) Farha, O. K.; Yazaydin, A. O.; Eryazici, I.; Malliakas, C. D.; Hauser, B. G.; Kanatzidis, M. G.; Nguyen, S. T.; Snurr, R. Q.; Hupp, J. T. *De Novo* Synthesis of a Metal−Organic Framework Material Featuring Ultrahigh Surface Area and Gas Storage Capacities. *Nat. Chem.* **2010**, *2*, 944−948.

(18) Yamada, K.; Tanaka, H.; Yagishita, S.; Adachi, K.; Uemura, T.; Kitagawa, S.; Kawata, S. Stepwise Guest Adsorption with Large Hysteresis in a Coordination Polymer $\{[Cu(bhnq)(THF)_2](THF)\}_n$ Constructed from a Flexible Hingelike Ligand. *Inorg. Chem.* **2006**, *45*, 4322−4324.

(19) Liu, X.; Li, Y.; Ban, Y.; Peng, Y.; Jin, H.; Bux, H.; Xu, L.; Caro, J.; Yang, W. Improvement of Hydrothermal Stability of Zeolitic Imidazolate Frameworks. *Chem. Commun.* **2013**, *49*, 9140−9142.

(20) Jiang, J. X.; Cooper, A. I. Microporous Organic Polymers: Design, Synthesis, and Function. *Top Curr Chem.* **2010**, *293*, 1−33.

(21) Zhang, Y.; Riduan, S. N. Functional Porous Organic Polymers for Heterogeneous Catalysis. *Chem. Soc. Rev.* **2012**, *41*, 2083−2094.

(22) Wan, J.-L.; Wang, C.; deKrafft, K. E.; Lin, W. Cross-Linked Polymers with Exceptionally High $Ru(bipy)_3^{2+}$ Loadings for Efficient Heterogeneous Photocatalysis. *ACS Catal.* **2012**, *2*, 417−424.

(23) Li, J.-R.; Tao, Y.; Yu, Q.; Bu, X.-H.; Sakamto, H.; Kitagawa, S. Selective Gas Adsorption and Unique Structural Topology of a Highly Stable Guest-Free Zeolite-Type MOF Material with N-Rich Chiral Open Channels. *Chem.—Eur. J.* **2008**, *14*, 2771−2776.

(24) Wu, H.; Reali, R. S.; Smith, D. A.; Trachtenberg, M. C.; Li, J. Highly Selective CO_2 Capture by a Flexible Microporous Metal−Organic Framework (MMOF) Material. *Chem.—Eur. J.* **2010**, *16*, 13951−13954.

(25) Maji, T. K.; Matsuda, R.; Kitagawa, S. A Flexible Interpenetrating Coordination Framework with a Bimodal Porous Functionality. *Nat. Mater.* **2007**, *6*, 142−148.

(26) Liu, Y.; Wang, Z. U.; Zhou, H.-C. Recent Advances in Carbon Dioxide Capture with Metal-Organic Frameworks. *Greenhouse Gases: Sci. Technol.* **2012**, *2*, 239−259.

(27) Horike, S.; Kishida, K.; Watanabe, Y.; Inubushi, Y.; Umeyama, D.; Sugimoto, M.; Fukushima, T.; Inukai, M.; Kitagawa, S. Dense Coordination Network Capable of Selective CO_2 Capture from C1 and C2 Hydrocarbons. *J. Am. Chem. Soc.* **2012**, *134*, 9852−9855.

(28) Du, N.; Park, H. B.; Robertson, G. P.; Dal-Cin, M. M.; Visser, T.; Scoles, L.; Guiver, M. D. Polymer Nanosieve Membranes for CO_2-Capture Applications. *Nat. Mater.* **2011**, *10*, 372−375.

(29) Rao, K. V.; Mohapatra, S.; Kulkarni, C.; Maji, T. K.; George, S. J. Extended Phenylene based Microporous Organic Polymers with Selective Carbon Dioxide Adsorption. *J. Mater. Chem.* **2011**, *21*, 12958−12963.

(30) Katsoulidis, A. P.; Kanatzidis, M. G. Phloroglucinol Based Microporous Polymeric Organic Frameworks with -OH Functional Groups and High CO_2 Capture Capacity. *Chem. Mater.* **2011**, *23*, 1818−1824.

(31) Lan, J.; Cao, D.; Wang, W.; Smit, B. Doping of Alkali, Alkaline-Earth, and Transition Metals in Covalent-Organic Frameworks for Enhancing CO_2 Capture by First-Principles Calculations and Molecular Simulations. *ACS Nano* **2010**, *4*, 4225−4237.

(32) Pandey, P.; Katsoulidis, A. P.; Eryazici, I.; Wu, Y.; Kanatzidis, M. G.; Nguyen, S. T. Imine-Linked Microporous Polymer Organic Frameworks. *Chem. Mater.* **2010**, *22*, 4974−4979.

(33) Jeon, H. J.; Choi, J. H.; Lee, Y.; Choi, K. M.; Park, J. H.; Kang, J. K. Highly Selective CO_2-Capturing Polymeric Organic Network Structures. *Adv. Energy Mater.* **2012**, *2*, 225−228.

(34) Xu, C.; Hedin, N. Synthesis of Microporous Organic Polymers with High CO_2-over-N_2 Selectivity and CO_2 Adsorption. *J. Mater. Chem. A* **2013**, *1*, 3406−3414.

(35) Dawson, R.; Cooper, A. I.; Adams, D. J. Chemical Functionalization Strategies for Carbon Dioxide Capture in Microporous Organic Polymers. *Polym. Int.* **2013**, *62*, 345−352.

(36) Song, W.-C.; Xu, X.-K.; Chen, Q.; Zhuang, Z.-Z.; Bu, X.-H. Nitrogen-Rich Diaminotriazine-Based Porous Organic Polymers for Small Gas Storage and Selective Uptake. *Polym. Chem.* **2013**, *4*, 4690−4696.

(37) Frisch, M. J. et al. *GAUSSIAN09, Revision D.01*; Gaussian Inc.: Wallingford, CT, 2009.

(38) Dennington, R.; Keith, T.; Millam, J. *GaussView, Version 5.0*; Semichem Inc.: Shawnee Mission, KS, 2009.

(39) Humphrey, W.; Dalke, A.; Schulten, K. VMD: Visual Molecular Dynamics. *J. Mol. Graphics* **1996**, *14*, 33−38.
(40) Van Gorp, J. J.; Vekemans, J.; Meijer, E. W. C_3-Symmetrical Supramolecular Architectures: Fibers and Organic Gels from Discotic Trisamides and Trisureas. *J. Am. Chem. Soc.* **2002**, *124*, 14759−14769.
(41) Suzuki, M.; Nakajima, Y.; Yumoto, M.; Kimura, M.; Shirai, H.; Hanabusa, K. Effects of Hydrogen Bonding and van der Waals Interactions on Organogelation Using Designed Low-Molecular-Weight Gelators and Gel Formation at Room Temperature. *Langmuir* **2003**, *19*, 8622−8624.
(42) Chen, Q.; Wang, J.-X.; Yang, F.; Zhou, D.; Bian, N.; Zhang, X.-J.; Yan, C.-G.; Han, B.-H. Tetraphenylethylene-Based Fluorescent Porous Organic Polymers: Preparation, Gas Sorption Properties and Photoluminescence Properties. *J. Mater. Chem.* **2011**, *21*, 13554−13560.
(43) Cote, A. P.; Benin, A. I.; Ockwig, N. W.; O'Keeffe, M.; Matzger, A. J.; Yaghi, O. M. Porous, Crystalline, Covalent Organic Frameworks. *Science* **2005**, *310*, 1166−1170.
(44) Wan, S.; Guo, J.; Kim, J.; Ihee, H.; Jiang, D. A Belt-Shaped, Blue Luminescent, and Semiconducting Covalent Organic Framework. *Angew. Chem., Int. Ed.* **2008**, *47*, 8826−8830.
(45) Zhao, Y.; Truhlar, D. G. The M06 Suite of Density Functionals for Main Group Thermochemistry, Thermochemical Kinetics, Noncovalent Interactions, Excited States, and Transition Elements: Two New Functionals and Systematic Testing of Four M06-Class Functionals and 12 Other Functionals. *Theor. Chem. Acc.* **2008**, *120*, 215−241.
(46) Dubinin, M. M. The Potential Theory of Adsorption of Gases and Vapors for Adsorbents with Energetically Nonuniform Surfaces. *Chem. Rev.* **1960**, *60*, 235−241.
(47) Zhao, Y.-C.; Wang, T.; Zhang, L.-M.; Cui, Y.; Han, B.-H. Facile Approach to Preparing Microporous Organic Polymers through Benzoin Condensation. *ACS Appl. Mater. Interfaces* **2012**, *4*, 6974−6981.
(48) Patel, H. A.; Karadas, F.; Byun, J.; Park, J.; Deniz, E.; Canlier, A.; Jung, Y.; Atilhan, M.; Yavuz, C. T. Highly Stable Nanoporous Sulfur-Bridged Covalent Organic Polymers for Carbon Dioxide Removal. *Adv. Funct. Mater.* **2013**, *23*, 2270−2276.
(49) Vaidhyanathan, R.; Iremonger, S. S.; Dawson, K. W.; Shimizu, G. K. H. An Amine-Functionalized Metal Organic Framework for Preferential CO_2 Adsorption at Low Pressures. *Chem. Commun.* **2009**, 5230−5232.
(50) Hasegawa, S.; Horike, S.; Matsuda, R.; Furukawa, S.; Mochizuki, K.; Kinoshita, Y.; Kitagawa, S. Three-Dimensional Porous Coordination Polymer Functionalized with Amide Groups Based on Tridentate Ligand: Selective Sorption and Catalysis. *J. Am. Chem. Soc.* **2007**, *129*, 2607−2614.
(51) Park, J.; Li, J.-R.; Chen, Y.-P.; Yu, J.; Yakovenko, A. A.; Wang, Z. U.; Sun, L.-B.; Balbuena, P. B.; Zhou, H.-C. A Versatile Metal−Organic Framework for Carbon Dioxide Capture and Cooperative Catalysis. *Chem. Commun.* **2012**, *48*, 9995−9997.
(52) Rao, K. V.; Mohapatra, S.; Maji, T. K.; George, S. J. Guest-Responsive Reversible Swelling and Enhanced Fluorescence in a Super-Absorbent, Dynamic Microporous Polymer. *Chem.—Eur. J.* **2012**, *18*, 4505−4509.